ELSEVIER

Science and Technology of Advanced Materials 7 (2006) 119–126

SCIENCE AND TECHNOLOGY OF ADVANCED MATERIALS

www.elsevier.com/locate/stam

# Thermodynamic modeling of the Ca–Ni system

D. Uremovich, F. Islam, M. Medraj *

*Concordia University, Montreal, Que., Canada*

Received 29 August 2005; received in revised form 25 September 2005; accepted 11 October 2005

**Abstract**

An interest in the binary Ca–Ni system has occurred due to the possibility of using this alloy system in hydrogen storage for fuel cell applications. A coherent database of thermodynamic properties pertaining to Ca–Ni will allow for easy access to a myriad of information. Using the published phase diagram and thermodynamic data of Ca–Ni from different sources, an optimized thermodynamic model is obtained. The model provides a means for a variety of other thermodynamic properties, for which no experimental data exists, to be predicted. The Ca–Ni binary system is essential in any further development of ternary or higher order systems based on these elements. Consistency between calculated and published experimental thermodynamic values enforces the legitimacy of the findings.


*Keywords:* Thermodynamic modeling; Ca–Ni system; $CaNi_5$ compound; Hydrogen storage

## 1. Introduction

Ca–Ni binary alloys show promising utilization as materials for hydrogen storage applications in fuel cell powered vehicles. This is confirmed by a number of journal articles that explore the possibility of alloying Ca–Ni compounds with a third element for hydrogen storage applications [1,2]. Various sources state that $CaNi_5$ is an inexpensive material with a high capacity for hydrogen storage, but demonstrates poor cycling stability [3]. $CaNi_5$ has also been suggested for use in partial oxidation of methane [4]. Notin et al. [5] indicated that of the four linear compounds formed in the Ca–Ni system, among them $CaNi_5$ demonstrates the greatest potential as a hydrogen storage material and for use in sulfur elimination in steel production.

This has led to investigations of Ca–Ni use in ternary alloys such as Ca–Mg–Ni. Liang and Schultz [1] experimented with this ternary and concluded that under certain manufacturing conditions; the hydrogen storage capability of Ca–Mg–Ni enhances hydrogen storage capacity.

Further research of the Ca–Ni binary alloy system is needed to test the feasibility of its inclusion in a ternary or higher order system for hydrogen storage. A comprehensive database of the thermodynamic properties pertaining to this binary alloy system will make research of this material manageable. Limited sources of Ca–Ni thermodynamic experimental data exist, including enthalpy of mixing, activity, and partial Gibbs energy of mixing. These data, coupled with experimental phase diagram, can be used to create an optimized system of thermodynamic properties pertaining to Ca–Ni.

In this analysis, all available published experimental data related to the Ca–Ni binary system were used during the optimization process. Gibbs energy of formation is also calculated from the optimized parameters. The liquidus line of the calculated phase diagram is determined using Redlich–Kister model. Prior to optimization, all experimental data were examined and any conflicting data was objectionably eliminated from use in the optimization.

## 2. Literature review

### 2.1. Phase diagram

Two variations of the Ca–Ni phase diagram exist. The details of each phase diagram were explored and the most suitable option selected. The most contested detail of the phase diagram is the existence of congruent melting of $CaNi_5$.

Takeuchi et al. [6] created a phase diagram from differential thermal analysis (DTA) with a congruent melting

* Corresponding author. Address: Department of Mechanical and Industrial Engineering, Concordia University, 1455 de Maisonneuve Blvd West, Montreal, Que., Canada H3G 1M8. Tel.: +1 514 848 2424x3146; fax: +1 514 848 3175.

*E-mail address:* mmedraj@encs.concordia.ca (M. Medraj).

1468-6996/$ - see front matter © 2005 Elsevier Ltd. All rights reserved.
doi:10.1016/j.stam.2005.10.002

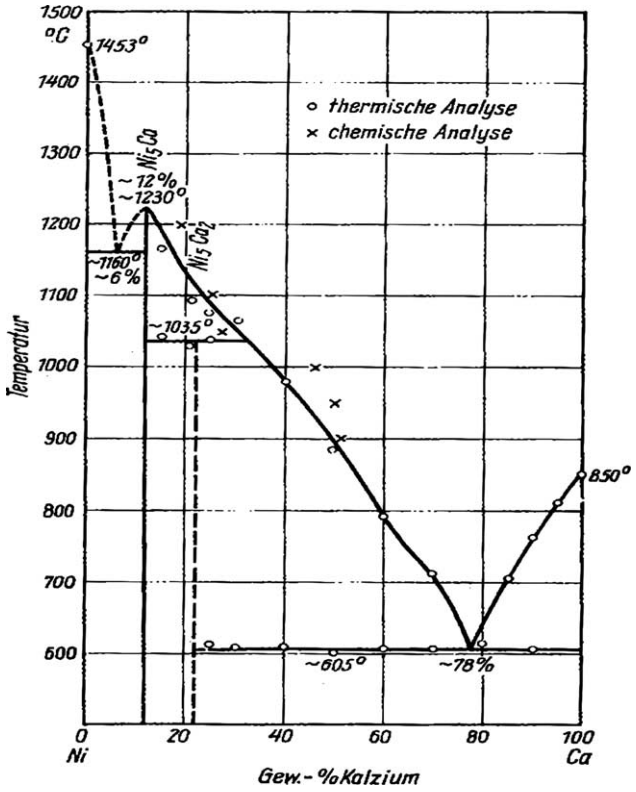


Fig. 1. Ca–Ni phase diagram Takeuchi et al. [6].

point at $CaNi_5$ and a eutectic line between this compound and Ni-fcc. A linear compound of $Ca_2Ni_5$ was also included in this initial phase diagram. This phase was also found by Dugdale [7]. The Ca–Ni phase diagram created by Takeuchi et al. is seen in Fig. 1.

Buschow [8] later determined the existence of the four intermetallic compounds with $CaNi_2$-cubic, $CaNi_3$-rhombohedral, $Ca_2Ni_7$-rhombohedral and $CaNi_5$-hexagonal crystal structure by X-ray diffraction. $Ca_2Ni_5$ was not found in this investigation and hence has been excluded from the further development of Ca–Ni phase diagrams.

From electrochemical measurements, Notin and Hertz [10] calculated the peritectic temperature of $CaNi_3$ and determined the thermodynamic properties of the solid compounds. Various sources including Saindrenan et al. [9] indicated that the melting of $CaNi_5$ occurs through a peritectic transformation. This suggestion and the experimental points related to the three other compounds according to Notin and Hertz [10] resulted in a newer version of the Ca–Ni phase diagram shown in Fig. 2. Okamoto [11] published a Ca–Ni phase diagram, which was based on data from Notin and Hertz [10] and Saindrenan et al. [9].

Notin et al. [5] explored the contested melting point of $CaNi_5$ and the possibility of it being peritectic or congruent in nature. A series of experiments by DTA on Ni-rich part finally suggested congruent melting of this compound and a eutectic point between $CaNi_5$ and Ni. Fig. 3 is the latest published phase diagram of Ca–Ni and has yet to be contested. The most recent optimized phase diagram has four linear compounds $CaNi_2$, $CaNi_3$, $Ca_2Ni_7$, and $CaNi_5$ and two eutectic points that occur at 896 and 1459 K. Three peritectic points at temperatures of 1139, 1287, and 1400 K. Also, it can be seen from this figure that $CaNi_5$ melts congruently at 1478 K.

The liquidus of Notin et al. [5] was used for the current optimization of the Ca–Ni system. In their work, the linear compound $CaNi_5$ terminates at around 850 K. This contradicts many of the previously published phase diagrams where all linear compounds are stable down to room temperature [6,11–13]. Besides, Notin et al. [5] did not include the phase transformation of Ca from FCC to BCC at 716 K. This phase transformation is shown by Okamoto [11] and can

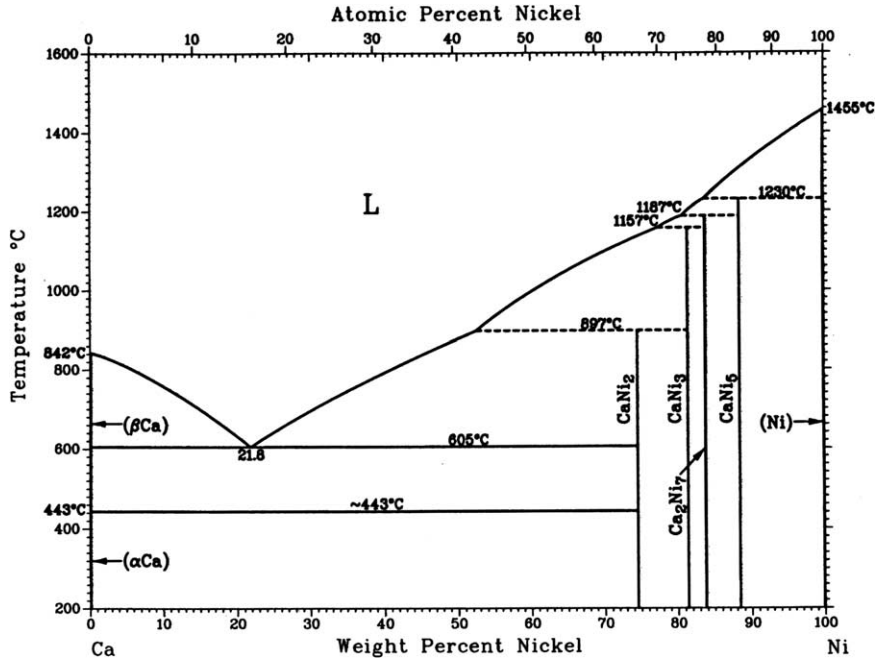


Fig. 2. Ca–Ni phase diagram Okamoto [11].

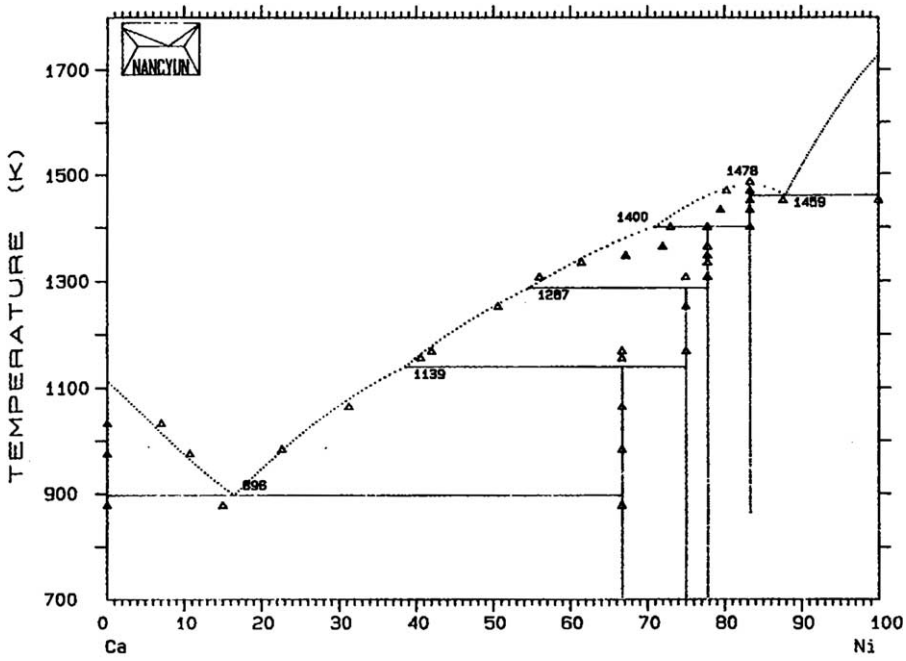


Fig. 3. Ca–Ni phase diagram Notin et al. [5].

be seen in Fig. 2. It is also stated by Callister [14] that at room temperature Ca exists as FCC structure.

### 2.2. Thermodynamic data

The amount of existing experimental thermodynamic data is limited. Sommer et al. [15] presented experimental enthalpy of mixing at a Ni concentration between 0 and 37%. Notin et al. [5] reported the optimized phase diagram with calculated enthalpy and entropy of mixing. Predel [13] compared the experimental data of enthalpy of mixing from Sommer et al. [15] and enthalpy of mixing calculated from Notin et al. [5] and concluded that these two sets of data do not match.

Meysson et al. [16] developed a series of partial activity values of calcium, which did not resemble the typical form of a partial activity curve. Hultgren et al. [17] extracted data points for partial activity of Ca by vapor pressure measurements and formed a feasible curve. They used the Gibbs–Duhem relation to determine the partial activity of Ni. Hultgren et al. [17] also calculated partial Gibbs energies from the partial activities found by Meysson et al. [16].

Notin et al. [5] calculated the entropy of mixing from the data used to calculate the most recent Ca–Ni phase diagram. Notin and Hertz [10] reported the enthalpy of formation, entropy of formation, and Gibbs energy of formation of the compounds in this system.

Although Notin et al. [5] worked on the Ca–Ni system elaborately but still there is some incompleteness. First, in their optimized phase diagram the stoichiometric compound $CaNi_5$ was not stable down to room temperature and second the phase transformation of Ca from Ca–fcc to Ca–bcc was absent. Moreover, the calculated enthalpy of mixing data reported by Notin et al. [5] contradicted with experimental work of Sommer et al. [15]. Hence, the reassessment is necessary to provide a self-consistent thermodynamic model, which reproduces the most acceptable phase diagram as well as the thermodynamic properties of this system.

## 3. Thermodynamic models

The optimum accuracy of phase diagram modeling is obtained if all experimental data are taken into account and if thermodynamic consistency exists between all thermodynamic functions of the different phases and the phase diagram. If these functions are presented analytically, they can be extrapolated for systems with one additional component. If the analytical representation always uses the same standardized models, all the information of a system will be contained in a set of coefficients and easily stored [18].

A system is at equilibrium when its Gibbs energy is at minimum. If we could calculate the Gibbs energy of all the possible phases of a system at a specified temperature as a function of composition, it would be a simple matter to select that phase or combination of phases, which provides the lowest value of Gibbs energy for that system. By definition, these would be the equilibrium phases for the system at that temperature. By repetition of these calculations for the number of temperatures, the phase boundaries of the system can be determined and the phase diagram can be constructed [19]. Once the binary subsystems have been analyzed by a coupled thermodynamic/phase diagram analysis, the phase diagram of a ternary or a quaternary system can usually be calculated with a maximum error within the uncertainty limits of the

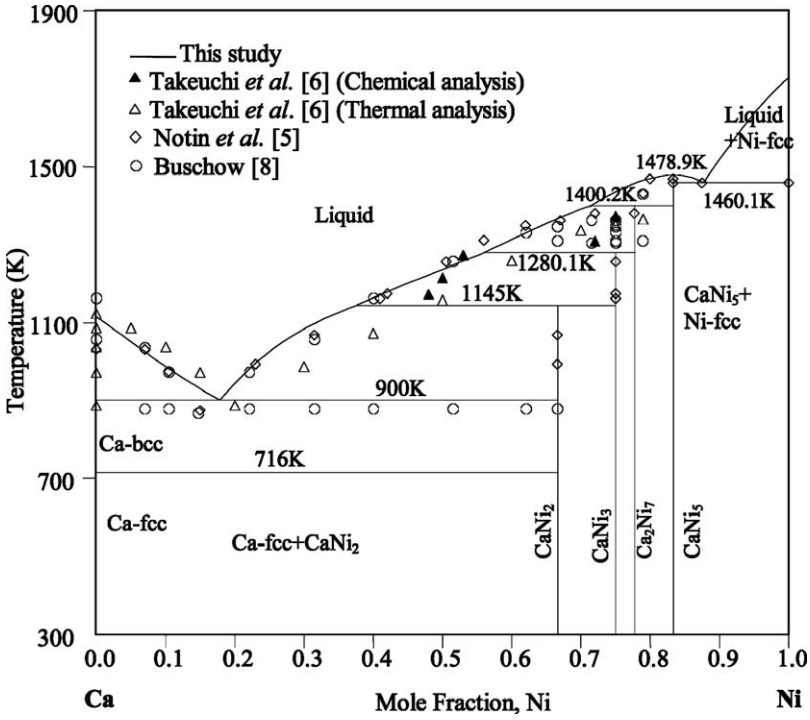


Fig. 4. Optimized Ca–Ni phase diagram.

experimental results, assuming that there are no strong ternary or quaternary interactions. Hence, in order to minimize the experimental effort, one should concentrate on re-measuring regions of the binary diagrams where required. The ternaries and quaternaries can then be recalculated [20].

$$G = \sum_{i=1}^{p} n_i G_i \tag{1}$$

For the calculation of phase equilibria in a multi-component system, it is necessary to minimize the total Gibbs energy, $G$, of all the phases that take part in this equilibrium where $n_i$ is the number of moles of phase $i$, $G_i$ is the Gibbs energy of phase $i$ and $p$ is the number of phases. All calculations, in this study, were performed with the aid of the WinPhaD thermodynamic computer software [21].

Table 1
Comparison of experimental and calculated liquidus points

| Type | Reaction | $X_{Ni}$-liquid | Temp. (K) | Ref. |
|---|---|---|---|---|
| Eutectic | Liquid → Ca-bcc + | 0.150 | 879.0 | [6] |
| | $CaNi_2$ | 0.170 | 900.0 | This work |
| Eutectic | Liquid → | 0.876 | 1451.0 | [5] |
| | Ni-fcc + $CaNi_5$ | 0.877 | 1460.1 | This work |
| Peritectic | Liquid + $CaNi_3$ → | 0.420 | 1170 | [10] |
| | $CaNi_2$ | 0.378 | 1145.0 | This work |
| Peritectic | Liquid + $Ca_2Ni_7$ → | 0.560 | 1308 | [8] |
| | $CaNi_3$ | 0.561 | 1280.1 | This work |
| Peritectic | Liquid + $CaNi_5$ → | 0.730 | 1401 | [5] |
| | $Ca_2Ni_7$ | 0.715 | 1400.2 | This work |
| Congruent | Liquid → $CaNi_5$ | 0.833 | 1484 | [5] |
| | | 0.833 | 1478.9 | This work |

### 3.1. Pure elements

Gibbs energy of a pure element ($i$), and phase ($\phi$), is represented by the following equations

$${}^{0}G_i^{\phi}(T) = G_i^{\phi}(T) - H_i^{\mathrm{SER}} \tag{2}$$

$${}^{0}G_i^{\phi} = a + bT + cT\ln T + dT^2 + eT^3 + fT^{-1} + gT^7 + hT^{-9} \tag{3}$$

where, $H_i^{\mathrm{SER}}$ is the molar enthalpy of stable element at a temperature of 298.15 K and pressure of 1 atm. The coefficients $a$ to $h$ are to be optimized.

### 3.2. Liquid solution phase

Gibbs energy of a liquid phase is represented by the following equation

Table 2
Optimized parameters of the Ca–Ni liquid

| Phase | Parameter | $a$ (J/g-atom) | $b$ (J/g-atom) |
|---|---|---|---|
| Liquid | $l_0$ | −25023.0 | 15.13 |
| | $l_1$ | 13652.58 | −1.91 |
| | $l_2$ | −6362.16 | −4.05 |
| $CaNi_2$ | $\Delta G_f$ | −7347.86 | 0.717 |
| $CaNi_3$ | $\Delta G_f$ | −7197.58 | 0.358 |
| $Ca_2Ni_7$ | $\Delta_f G$ | −7047.45 | 0.2856 |
| $CaNi_5$ | $\Delta G_f$ | −5998.24 | ~0 |
| Ca-fcc[a] | $\Delta G_f$ | 0 | 0 |
| Ca-bcc[a] | $\Delta G_f$ | 0 | 0 |
| Ni-fcc[a] | $\Delta G_f$ | 0 | 0 |

[a] In this study, the lattice stability values are not added to ΔG° of the pure elements Ca–fcc, Ca–bcc and Ni-fcc.

Table 3
Optimized Gibbs energy of formation parameters for the linear compounds

| Gibbs energy of formation | Temp. (K) | $CaNi_2$ | $CaNi_3$ | $Ca_2Ni_7$ | $CaNi_5$ |
|---|---|---|---|---|---|
| $\Delta G_f$ (J/g-atom) | 1050 | −6595.01 | −6821.68 | −6747.57 | −5997.24 |
| | 1200 | −6487.46 | −6767.98 | −6704.73 | −5997.24 |
| | 1350 | −6379.91 | −6714.28 | −6661.89 | −5997.24 |

$$G = x_i^0 G_i^\phi + x_j^0 G_j^\phi + \mathrm{RT}[x_i \ln x_i + x_j \ln x_j] + {}^{ex}G^\phi \quad (4)$$

where, $\phi$ is the phase, $x_i$ is the mole fraction of component $i$, $x_j$ is the mole fraction of component $j$, $x_i^0 G_i^\phi + x_j^0 G_j^\phi$ is the Gibbs energy of mechanical mixture, $\mathrm{RT}[x_i \ln x_i + x_j \ln x_j]$ is the ideal Gibbs energy, and ${}^{ex}G^\phi$ is the excess Gibbs energy.

The excess Gibbs energy can be represented by Redlich–Kister polynomials

$${}^{ex}G^\phi = x_i x_j \sum_{n=0}^{n=m} {}^{n}L_{i,j}^\phi (x_i - x_j)^n \quad (5)$$

where, ${}^{n}L_{i,j}^\phi$ are the polynomial coefficients and can be written as ${}^{n}L_{i,j}^\phi = a_n + b_n \times T$, $(n = 0,\ldots,m)$ and $a_n$, $b_n$ are the parameters to be optimized and stored in a database for this system.

### 3.3. Linear compound phase

Gibbs energy of stoichiometric compounds is represented by the following equation

$$G^\phi = x_i^0 G_i^{\phi_1} + x_j^0 G_j^{\phi_2} + \Delta G_f \quad (6)$$

where, $\Delta G_f = a + bT$, $x_i$ is the mole fraction of component $i$, $x_j$ is the mole fraction of component $j$, ${}^0G_i^{\phi_1}$ and ${}^0G_j^{\phi_2}$ are the Gibbs energy of an element in its standard state.

## 4. Results and discussion

### 4.1. Phase diagram

Fig. 4 shows the calculated Ca–Ni phase diagram in relation with experimental data from the literature. A good agreement with the liquidus line between the calculated values in this work and experimental values of Notin et al. [5] and Buschow [8] is found in Fig. 4. However, the results reported by Takeuchi et al. [6] contradict with the calculated values in this study because they [6] reported only two intermetallic compounds $CaNi_5$ and $Ca_2Ni_5$ instead of four. All points on the calculated phase diagram are within approximately 0.02 mol fraction of the experimental points determined by Notin et al. [5]. A comparison of calculated and experimental results of the critical regions of the Ca–Ni phase diagram is shown in Table 1.

Phase transformation of Ca from FCC to BCC is evident in this diagram. This was not included in Notin et al. [5]. Furthermore, this diagram shows that the $CaNi_5$ compound is stable down to room temperature unlike the phase diagram reported by Notin et al. [5].

Three Redlich–Kister coefficients were required to model the liquid phase and to calculate the most optimal phase diagram and thermodynamic properties. These coefficients are listed in Table 2. Lattice stability values were not added to Ca-fcc and Ca-bcc and Ni-fcc phases, this enables combining the current description with other systems in a multi-component thermodynamic database.

The reference states of the Gibbs energy of formation for the four intermetallic compounds are considered as Ni-fcc and Ca-bcc. Optimum values of Gibbs energy of formation were obtained and can be seen in Table 3.

The values in Table 3 are close to those reported by Notin and Hertz [10]. A comparison between Gibbs energies of formation of the stoichiometric compounds in this system published by Notin and Hertz [10] and those calculated in this work can be seen in the Fig. 5. This figure shows that the

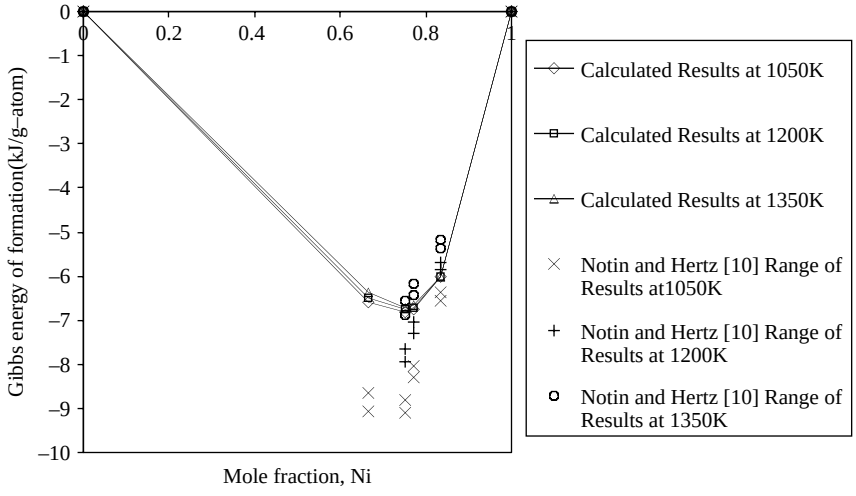


Fig. 5. Comparison between the calculated Gibbs energy of formation and experimental results from the literature.

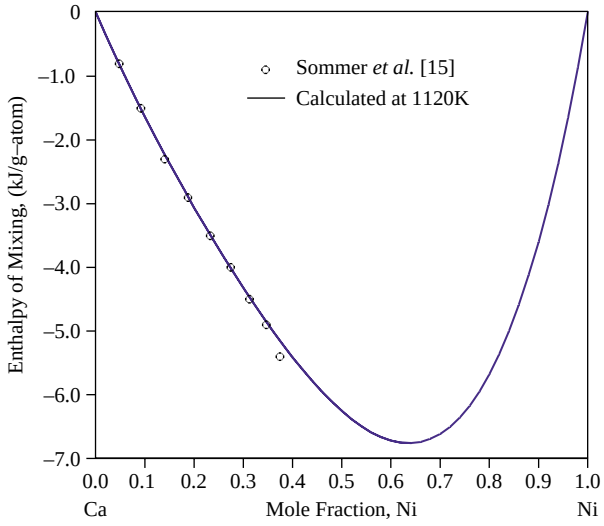


Fig. 6. Enthalpy of mixing of liquid Ca–Ni at 1120 K.

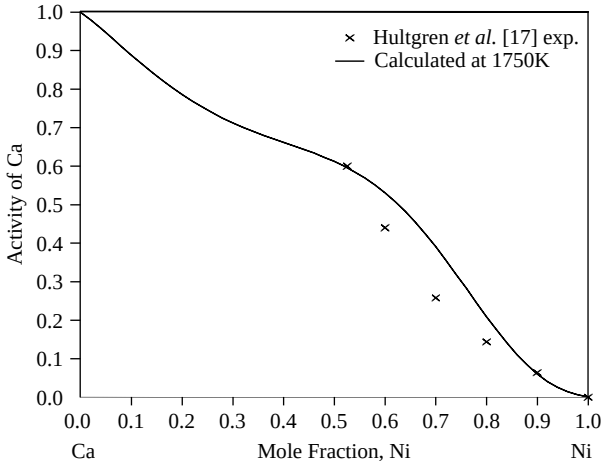


Fig. 7. Activity of Ca in liquid Ca–Ni at 1750 K.

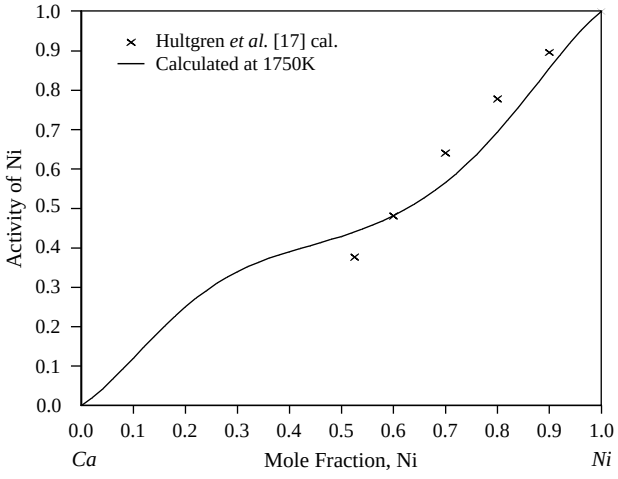


Fig. 8. Activity of Ni in liquid Ca–Ni at 1750 K.

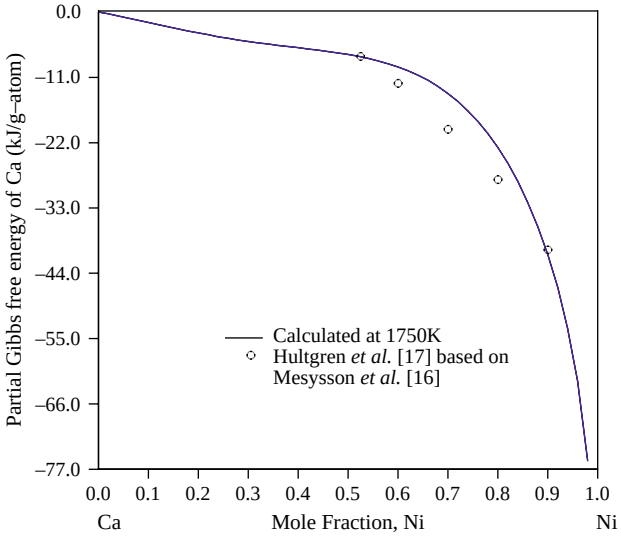


Fig. 9. Gibbs partial energy of Ca at 1750 K.

calculated values presented in the current analysis are consistent with those reported by [10].

### 4.2. Thermodynamic properties

The data of enthalpy of mixing by Sommer et al. [15] was used in the optimization and matched the calculated enthalpy of mixing curve seen in Fig. 6. Ozturk et al. [22] mentioned that the binary system with alkaline earth elements that has intermetallic compounds whose melting temperatures are much higher than those of the constituents elements will have a deep valley in the enthalpy of mixing. In this system, there is asymmetric deep valley in the curve of the enthalpy of mixing (Fig. 6). The lowest point of the curve is shifted towards Ni-rich side where the intermetallic compounds are formed. This shift indicates stronger atomic interactions in the liquid at the composition of the intermetallic compounds.

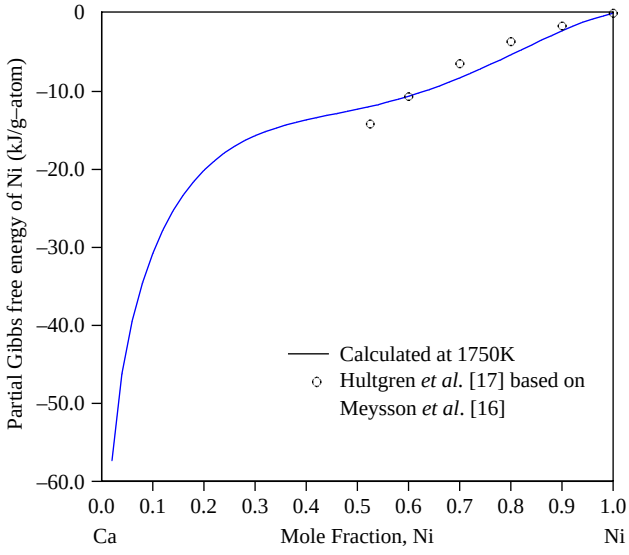


Fig. 10. Gibbs partial energy of Ni at 1750 K.

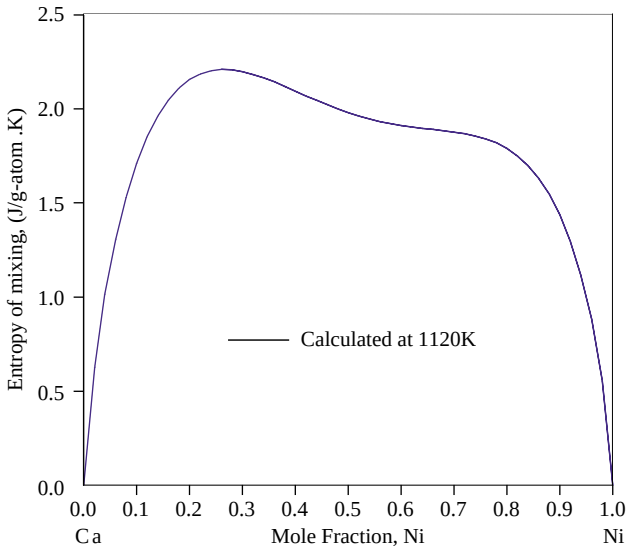


Fig. 11. Entropy of mixing of liquid Ca–Ni at 1120 K.

The activities of Ca and Ni published by Hultgren et al. [17] were used in the optimization of the Ca–Ni system. Comparison between the calculated activity of Ca and Ni from [17] is shown in Figs. 7 and 8, respectively. The experimental partial activities at 1750 K followed the general trend of the calculated values. Although a deviation exists between calculated and experimental data, an exact match is often very difficult to obtain. Only one set of experimental data is available for comparison with the calculated curve. This sets up the possibility that the deviation is within the uncertainty limits of the measured values especially since these data were obtained by vapor pressure measurements which usually show large degree of scatter. The system having such negative enthalpy of mixing (shown in Fig. 6) with activity plots similar to the ideal one is unusual. This means that the excess entropy just happens to nearly balance out the excess enthalpy at 1750 K temperature at which activities are measured.

Figs. 9 and 10 show that calculated partial Gibbs energies followed the same trend as the experimental results from the literature. These values were not included in the optimization and are predicted by the developed model, which in turn proves the quality of the model.

The calculated entropy of mixing of the liquid phase is shown in Fig. 11. Experimental data are not available in the literature for this. It is evident that the calculated entropy of mixing of the liquid phase at 1120 K shows a lower value in the Ni rich part roughly near the composition where the enthalpy of mixing is minimum indicating a tendency for short range order in the Ni–Ca liquid.

## 5. Conclusion

- Thermodynamic description for the Ca–Ni binary system has been obtained.
- The values of the model parameters of Ca–Ni system are obtained by optimization using known phase equilibrium and thermodynamic data. The present work provides self-consistent model, which can be used for higher order systems.
- Minimum number of optimized thermodynamic coefficients was used to calculate phase diagram and other integral and partial thermodynamic properties such as activities, enthalpy of mixing, partial Gibbs free energy, which reproduced the experimental values very well.
- The optimized model parameters can also be used to predict thermodynamic properties, which might not be available in the literature. For instance partial Gibbs energy of mixing was predicted by the current model and coincided with the experimental data, which were not used for the optimization.
- It is possible to sustain an optimized Ca–Ni system where $CaNi_5$ is stable down to room temperature and Ca experiences phase transformation from FCC to BCC at 716 K.

## References

[1] G. Liang, R. Schulz, Phase structures and hydrogen storage properties of Ca–Mg–Ni alloys prepared by mechanical alloying, J. Alloys Compd. 356–357 (1–2) (2003) 612–616.
[2] J.O. Jensen, N.J. Bjerrum, Systematic B-metal substitution in $CaNi_5$, J. Alloys Compd. 293–295 (1–2) (1999) 185–189.
[3] P.D. Goodell, Stability of rechargeable hydriding alloys during extended cycling, J. Less-Common Met. 99 (1) (1984) 1–14.
[4] J.H. Jun, T.J. Lee, T.H. Lim, S.W. Nam, S.A. Hong, K.J. Yoon, Nickel–calcium phosphate/hydroxyapatite catalysts for partial oxidation of methane to syngas: characterization and activation, J. Catal. 221 (1) (2004) 178–190.
[5] M. Notin, D. Belbacha, M. Rahmane, J. Hertz, G. Saindrenan, J.L. Jorda, Experimental diagram and numerical optimization of the calcium–nickel system, J. Less-Common Met. 162 (2) (1990) 221–229.
[6] Y. Takeuchi, K. Mochizuki, M. Watanabe, I. Obinata, Alloys of nickel with alkali and alkali-earth metals, Metallurgy 20 (1) (1966) 2–8.
[7] P.J. Dugdale, Thermodynamics of the calcium–nickel system by atomic absorption spectrophotometry, Thesis, 1976.
[8] K.H.J. Buschow, Calcium–nickel intermetallic compounds, J. Less-Common Met. 38 (1974) 95–98.
[9] G. Saindrenan, J. Vitart-Barbier, M. Constantinoff, Structural study of nickel–calcium alloys between 0 and 15 wt% calcium, J. Less-Common Met. 118 (2) (1986) 227–333.
[10] M. Notin, J. Hertz, Potentiometric study of thermodynamic properties of calcium–nickel intermetallic compounds. Structure interpretation, Acta Metall. 31(6) (1983) 903–908.
[11] T.B. Massalski, Binary Alloy Phase Diagram, ASM International, Metals Park, 1991.
[12] W.G. Moffatt, The Handbook of Binary Phase Diagrams, ASM International, Metals Park, 1986.
[13] B. Predel, Landolt-Bornstein, Group IV: Physical Chemistry: Phase Equilibria, Crystallographic Data and Values of Thermodynamic Properties of Binary Alloys: Subvolume C, Springer/GMBH & Co., Berlin/Heidelberg, Germany, 1991.
[14] W.D. Callister Jr., Materials Science and Engineering and Introduction, fifth ed., Wiley, New York, 2000.
[15] F. Sommer, J.J. Lee, B. Predel, Thermodynamic studies of liquid aluminum–calcium, aluminum–strontium, magnesium–nickel, and calcium–nickel alloys, Z. Metallkde. 74 (2) (1983) 100–104.
[16] N. Meysson, A. Rist, Measurement of calcium activity in molten nickel–calcium and iron–nickel–calcium alloys, Rev. Met. 62 (1965) 1127–1131.

[17] R. Hultgren, P. Desai, D. Hawkins, M. Gleiser, K. Kelley, Selected Values of the Thermodynamic Properties of Binary Alloys, ASM International, Metals Park, 1973.
[18] H.L. Lukas, E. Henig Th., B. Zimmermann, Optimization of phase diagrams by a least squares method using simultaneously different types of data, Calphad 3 (1977) 225–236.
[19] Bergeron, Risbud, Introduction to Phase Equilibria in Ceramics, The American Ceramic Society, Westerville, 1984.
[20] W. Bale, D. Pelton, Coupled phase diagram and thermodynamic analysis of the 18 binary systems formed among $Li_2CO_3$, $K_2CO_3$, $Na_2CO_3$, LiOH, KOH, NaOH, $Li_2SO_4$, $K_2SO_4$ and $Na_2SO_4$, Calphad 4 (6) (1982) 253–278.
[21] WinPhaD—Phase diagram calculation engine for multi component systems, CompuTherm LLC, Madison, WI, 2000.
[22] K. Ozturk, L.-Q. Chen, Z.-K. Liu, Thermodynamic assessment of the Al–Ca binary system using random solution and associate models, J. Alloys Compd. 340 (1–2) (2002) 199–206.